DISPROVING THE THEORY OF LOCAL HIDDEN VARIABLES THROUGH OBSERVING THE COINCIDENCE OF ENTANGLED PHOTON PAIRS

J. PUGHE-SANFORD

Abstract. The theory of local hidden variables (HVT), believed to complete the picture of quantum mechanics by allowing for deterministic formulae, is investigated and ultimately disproven. More specifically, a photon beam is shone through a pair of BaB_2O_4 crystals to produce pairs of entangled photons, the coincidence of which through separate polarizers is measured. Malus' Law is experimentally confirmed for this system. Additionally, operators are defined for these polarizers and the expectation value of their product calculated in terms of their respective angles. An abstract quantity is then defined as a unique sum of these expectation values at four unique configurations. According to HVT, this quantity is constrained to $[-2, 2]$, while according to quantum mechanics (QM) it is not. Over two trials, this value was found to be $2.55 \pm .11$, disproving HVT as a viable explanation of the outcome of quantum processes.

1. Introduction

Since the conception of quantum mechanics, what determines the collapse of a wave function into a single observable state has troubled many physicists. To this day, QM has offered only a statistical explanation of these results. Classically, the behavior of all systems are theoretically deterministic if the initial state of the system is sufficiently known. This dissimilarity has lead many to develop theories that could explain, deterministically, the outcome of quantum processes. One such theory is the theory of local hidden variables, which supposes that there may be some variable that we cannot or have not yet detected, the value of which determines the state into which the quantum system collapses upon observation. Using Bell's theorem, it's possible to disprove the existence of such a variable, the methodology of which stems from observing entangled particles.

Consider a pair of entangled photons, labelled a and b, created by spontaneous parametric downconversion of a photon. These photons are distinguishable by the path they travel, as their paths are distinct. The state of this system exists in a superposition of two basis states, as both particles must have the same polarization. Thus, the system can be described as

$$|\phi\rangle = \cos\theta|h\rangle_a|h\rangle_b + \sin\theta|v\rangle_a|v\rangle_b,$$

for a photon of polarization θ undergoing spontaneous parametric downconversion, where $|v\rangle, |h\rangle$ define unit vectors along the vertically polarized and horizontally polarized axes. For $\theta = \frac{\pi}{2}$, this becomes

$$|\phi\rangle = \frac{1}{\sqrt{2}}|h\rangle_a|h\rangle_b + \frac{1}{\sqrt{2}}|v\rangle_a|v\rangle_b. \tag{1.1}$$

In this configuration, consider placing two polarizers along the paths of a and b positioned at angles α and β, respectively. The probability of observing the coincidence of both photons passing through their respective polarizers is

$$\begin{aligned} P_{TT}(\alpha,\beta) &= |\langle\alpha|_a\langle\beta|_b|\phi\rangle|^2 \\ &= \frac{1}{2}|\langle\alpha|_a\langle\beta|_b|h\rangle_a|h\rangle_b + \langle\alpha|_a\langle\beta|_b|v\rangle_a|v\rangle_b|^2 \\ &= \frac{1}{2}|\cos\alpha\cos\beta + \sin\alpha\sin\beta|^2 \\ &= \frac{1}{2}|\cos(\alpha-\beta)|^2 \\ &= \frac{1}{2}\cos^2(\alpha-\beta). \end{aligned} \tag{1.2}$$

This result is consistent with Malus' Law, which tells us that the intensity of polarized light on a detector is proportional to the square of the cosine of the angle between the polarizer and the polarization of the light. Thus, when one of the entangled photons is detected with polarization α, the likelihood of measuring a coincidence at the second detector is proportional to $\cos^2(\alpha-\beta)$, as shown above.

1.1. **Quantum Theory.** Note that the probability of both photons being transmitted can also be described in terms of the number of coincidences observed by the detector, $N(\alpha,\beta)$, over the total number of photon pairs that arrived at the polarizers N_{tot}.

$$P_{TT}(\alpha,\beta) = \frac{N(\alpha,\beta)}{N_{\text{tot}}}$$

Now N_{tot} is not explicitly measurable, given that it must be the total number of photons incident on the polarizers, even those that aren't transmitted by the polarizer, which we have no way of measuring. We can, however, construct N_{tot} from a collection of observable coincidences as

$$N_{\text{tot}} = N(\alpha,\beta) + N(\alpha,\beta+\frac{\pi}{2}) + N(\alpha+\frac{\pi}{2},\beta) + N(\alpha+\frac{\pi}{2},\beta+\frac{\pi}{2}).$$

Quite similarly, the probability of other outcomes, such as the photon being transmitted along path a but not along path b, P_{TE}, being transmitted along path b but not along path a, P_{ET}, or both being extinguished (not

transmitted), P_{EE}, can be described as

$$\begin{aligned} P_{TE}(\alpha,\beta) &= \frac{N(\alpha,\beta+\frac{\pi}{2})}{N_{\text{tot}}} \\ P_{ET}(\alpha,\beta) &= \frac{N(\alpha+\frac{\pi}{2},\beta)}{N_{\text{tot}}} \\ P_{EE}(\alpha,\beta) &= \frac{N(\alpha+\frac{\pi}{2},\beta+\frac{\pi}{2})}{N_{\text{tot}}}, \end{aligned}$$

which together form a normalized probability distribution.

The detection of these photons is determined at the moment of interaction with the polarizer. Thus, we will define a polarization operator $\hat{P}^{(\theta)}$ with eigenvalues 1 and -1 for transmitting or extinguishing a photon through a polarizer of angle θ, respectively. The expectation value of the observable quantity $\hat{P}_a^{(\alpha)}\hat{P}_b^{(\beta)}$ on an arbitrary $|\phi\rangle = h|h\rangle_a|h\rangle_b + v|v\rangle_a|v\rangle_b$ can be derived in terms of these probabilities by projecting $|\phi\rangle$ into the orthonormal basis,

$$\{|\alpha\rangle_a, |\alpha+\frac{\pi}{2}\rangle_a\} \otimes \{|\beta\rangle_b, |\beta+\frac{\pi}{2}\rangle_b\}.$$

This produces an equation for $|\phi\rangle$ that diagonalizes $\hat{P}_a^{(\alpha)}\hat{P}_b^{(\beta)}$,

$$\begin{aligned} |\phi'\rangle &= (\langle\alpha|_a\langle\beta|_b + \langle\alpha+\frac{\pi}{2}|_a\langle\beta|_b + \langle\alpha|_a\langle\beta+\frac{\pi}{2}|_b + \langle\alpha+\frac{\pi}{2}|_a\langle\beta+\frac{\pi}{2}|_b)|\phi\rangle \\ &= (h\langle\alpha|h\rangle_a\langle\beta|h\rangle_b + v\langle\alpha|v\rangle_a\langle\beta|v\rangle_b)|\alpha\rangle_a|\beta\rangle_b \\ &+ (h\langle\alpha+\frac{\pi}{2}|h\rangle_a\langle\beta|h\rangle_b + v\langle\alpha+\frac{\pi}{2}|v\rangle_a\langle\beta|v\rangle_b)|\alpha+\frac{\pi}{2}\rangle_a|\beta\rangle_b \\ &+ (h\langle\alpha|h\rangle_a\langle\beta+\frac{\pi}{2}|h\rangle_b + v\langle\alpha|v\rangle_a\langle\beta+\frac{\pi}{2}|v\rangle_b)|\alpha\rangle_a|\beta+\frac{\pi}{2}\rangle_b \\ &+ (h\langle\alpha+\frac{\pi}{2}|h\rangle_a\langle\beta+\frac{\pi}{2}|h\rangle_b + v\langle\alpha+\frac{\pi}{2}|v\rangle_a\langle\beta+\frac{\pi}{2}|v\rangle_b)|\alpha+\frac{\pi}{2}\rangle_a|\beta+\frac{\pi}{2}\rangle_b \\ &= (h\cos\alpha\cos\beta + v\sin\alpha\sin\beta)|\alpha\rangle_a|\beta\rangle_b \\ &+ (-h\sin\alpha\cos\beta + v\cos\alpha\sin\beta)|\alpha+\frac{\pi}{2}\rangle_a|\beta\rangle_b \\ &+ (-h\cos\alpha\sin\beta + v\sin\alpha\cos\beta)|\alpha\rangle_a|\beta+\frac{\pi}{2}\rangle_b \\ &+ (h\sin\alpha\sin\beta + v\cos\alpha\cos\beta)|\alpha+\frac{\pi}{2}\rangle_a|\beta+\frac{\pi}{2}\rangle_b \end{aligned}$$

such that,

$$\begin{aligned}\langle\phi'|\hat{P}_a^{(\alpha)}\hat{P}_b^{(\beta)}|\phi'\rangle &= (1)^2P_{TT}(\alpha,\beta)+(-1)(1)P_{ET}(\alpha,\beta)\\ &+ (1)(-1)P_{TE}(\alpha,\beta)+(-1)^2P_{EE}(\alpha,\beta)\end{aligned}$$

since

$$\begin{aligned}P_{TT}(\alpha,\beta) &= |h\cos\alpha\cos\beta+v\sin\alpha\sin\beta|^2\\ P_{TE}(\alpha,\beta) &= |-h\sin\alpha\cos\beta+v\cos\alpha\sin\beta|^2\\ P_{ET}(\alpha,\beta) &= |-h\cos\alpha\sin\beta+v\sin\alpha\cos\beta|^2\\ P_{EE}(\alpha,\beta) &= |h\sin\alpha\sin\beta+v\cos\alpha\cos\beta|^2.\end{aligned}$$

To reiterate, this expectation value is an observable quantity that measures the agreement of the measurements of the two polarizers, ranging from 1 when in agreement and -1 when in disagreement. We will call this quantity

$$E_{\mathrm{QM}}(\alpha,\beta)\equiv P_{TT}(\alpha,\beta)-P_{ET}(\alpha,\beta)-P_{TE}(\alpha,\beta)+P_{EE}(\alpha,\beta). \tag{1.3}$$

Taking the coefficients used in Equation 1.1, $v=h=\frac{1}{\sqrt{2}}$, this value reduces to

$$E_{\mathrm{QM}}(\alpha,\beta)=\cos[2(\alpha-\beta)] \tag{1.4}$$

1.2. **Theory of Hidden Variables.** The measurement of agreement between the polarizers can also be derived in terms of HVT. Given a hidden variable χ, we should now have a complete description of the state of the system, allowing us to define a function

$$A(\alpha,\chi)=\begin{cases}1 & \text{photon } a \text{ is measured at angle } \alpha\\ -1 & \text{photon } a \text{ is not measured at angle } \alpha\end{cases} \tag{1.5}$$

describing the outcome of the detector on path a. Similarly, we can define

$$B(\beta,\chi)=\begin{cases}1 & \text{photon } b \text{ is measured at angle } \beta\\ -1 & \text{photon } b \text{ is not measured at angle } \beta\end{cases} \tag{1.6}$$

for path b.

Given any probability distribution $\rho(\chi)$, the probabilities expressed through QM can be written in terms of A and B as

$$P_{TT}(\alpha,\beta) = \int\frac{1-A(\alpha,\chi)}{2}\frac{1-B(\beta,\chi)}{2}\rho(\chi)d\chi \tag{1.7}$$

$$P_{TE}(\alpha,\beta) = \int\frac{1-A(\alpha,\chi)}{2}\frac{1+B(\beta,\chi)}{2}\rho(\chi)d\chi \tag{1.8}$$

$$P_{ET}(\alpha,\beta) = \int\frac{1+A(\alpha,\chi)}{2}\frac{1-B(\beta,\chi)}{2}\rho(\chi)d\chi \tag{1.9}$$

$$P_{EE}(\alpha,\beta) = \int\frac{1+A(\alpha,\chi)}{2}\frac{1+B(\beta,\chi)}{2}\rho(\chi)d\chi. \tag{1.10}$$

Manipulating Equations 1.7−1.10, gives us the corollary of $E_{\text{QM}}(\alpha,\beta)$ within the context of HVT as

$$\begin{aligned} E_{\text{HVT}}(\alpha,\beta) &= \int \frac{\rho(\chi)d\chi}{4}[(1-A(\alpha,\chi))(1-B(\beta,\chi)) - (1-A(\alpha,\chi))(1+B(\beta,\chi)) \\ &\qquad -(1+A(\alpha,\chi))(1-B(\beta,\chi)) + (1+A(\alpha,\chi))(1+B(\beta,\chi))] \\ &= \int \frac{\rho(\chi)d\chi}{4}[4A(\alpha,\chi)B(\beta,\chi)] \\ &= \int A(\alpha,\chi)B(\beta,\chi)\rho(\chi)d\chi. \end{aligned}$$

From Equations 1.5 and 1.6, we can also construct the quantity s as

$$s = A(a,\chi))\left[B(b,\chi)) - B(b',\chi))\right] + A(a',\chi))\left[B(b,\chi)) + B(b',\chi))\right],$$

for angles a, a', b, and b'. Due to our definitions of A and B, s can either be 2 or -2.

1.3. **Expected Outcomes of QM vs HVT.** The subtlety of how the predictions of QM differ from those of HVT can be seen through a manipulation of the long term expectation value of s. In terms of HVT,

$$\begin{aligned} S_{\text{HVT}} &= \int s\rho(\chi)d\chi \\ &= \int A(a,\chi)\left[B(b,\chi) - B(b',\chi)\right] + A(a',\chi)\left[B(b,\chi) + B(b',\chi)\right]\rho(\chi)d\chi \\ &= \int A(a,\chi)B(b,\chi)\rho(\chi)d\chi - \int A(a,\chi)B(b',\chi)\rho(\chi)d\chi \\ &\quad + \int A(a',\chi)B(b,\chi)\rho(\chi)d\chi + \int A(a',\chi)B(b',\chi)\rho(\chi)d\chi \\ &= E_{\text{HVT}}(a,b) - E_{\text{HVT}}(a,b') + E_{\text{HVT}}(a',b) + E_{\text{HVT}}(a',b'). \end{aligned}$$

Given that s is either 2 or -2, its average must be confined to the interval $[-2,2]$. Dissimilarly, the value

$$S_{\text{QM}} = E_{\text{QM}}(a,b) - E_{\text{QM}}(a,b') + E_{\text{QM}}(a',b) + E_{\text{QM}}(a',b'), \tag{1.11}$$

is not bounded explicitly within this range. In fact, for constraints $a' = a + \frac{\pi}{4}$ and $b' = b + \frac{\pi}{4}$, S can be reduced using Equation 1.4 to

$$S_{\text{QM}} = 2\cos[2(a-b)] - 2\sin[2(a-b)],$$

which has a max of $S = 2.82843$ at $a - b = -\frac{\pi}{8} + 2\pi n$ or $\frac{3\pi}{8} + 2\pi n$, for $n \in \mathbb{Z}$. Observing such a value of S, outside $[-2,2]$, would disprove HVT.

2. Setup

We used 405 nm laser in this experiment, prepared at a polarization of 45° using a horizontal polarizer and half wave plate in series. We passed the beam through a pair of BaB_2O_4 crystals, causing the incoming photons to undergo spontaneous parametric downconversion and produce entangled

810 nm photon pairs. We placed a compensating crystal between the laser and the pair to ensure that both states of the photon system are in phase once spontaneous parametric downconversion occurs.

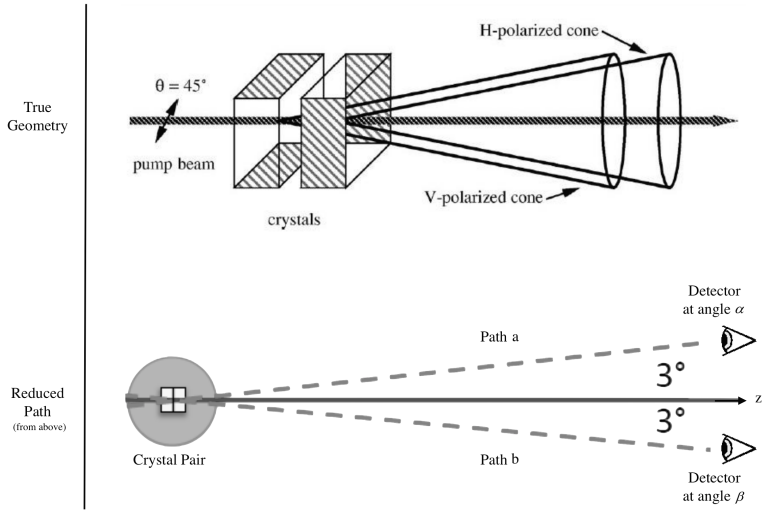

FIGURE 1. A visual description of restriction of this experiment to the vertical plane.[1]

As shown in Figure 1, the entangled photons are ejected along opposing edges of a cone whose vertex is the point of intersection with the crystal pair. As opposed to using an array of detectors around a circular cross-section of the cone, we constrained our detection of exiting photons to paths parallel to the optical table, placing collimators 38 in horizontally away from the crystal pair, 3° from the horizontal, along the edges of the cone. In front of these collimators, we placed 810 nm wave band filters to reduce the number of photons from environmental sources hitting our detectors, and fixed horizontal polarizers in front of those. As the polarizers used did not rotate themselves, half wave plates were placed in front of them to achieve the effect of rotation throughout the experiment.

We used fiber optic cables to feed the photons entering the collimators into the photon detectors. The outputs of the detectors were read by an FPGA looking for coincidences within a 25 ns window, the data for which was then logged using MatLab. FPGA and computer excluded, our construction of this setup can be seen in Figure 2.

It should be noted for clarity that the use of half waves plates rotates the photon beam around a fixed axis, meaning that every degree of rotation of the half wave plate is actually two degrees of rotation of the beam. For

[1]Images used in this graphic, from top to bottom, are from Dehlinger and Mitchell, Am. J. Phys. 70, 903-910 (2002) and Galvez, (Colgate University).

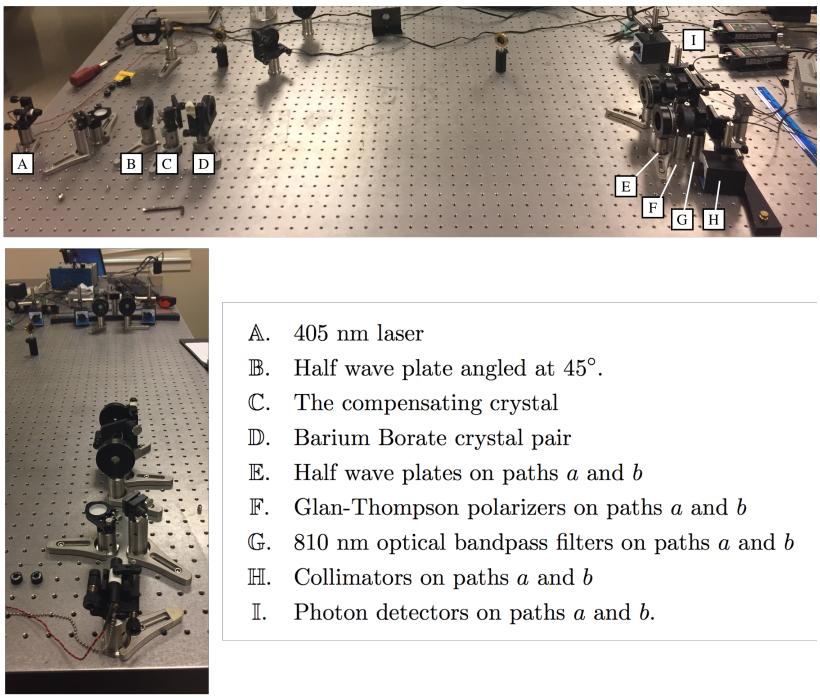

𝔸. 405 nm laser
𝔹. Half wave plate angled at 45°.
ℂ. The compensating crystal
𝔻. Barium Borate crystal pair
𝔼. Half wave plates on paths a and b
𝔽. Glan-Thompson polarizers on paths a and b
𝔾. 810 nm optical bandpass filters on paths a and b
ℍ. Collimators on paths a and b
𝕀. Photon detectors on paths a and b.

FIGURE 2. Labelled above is the setup used to in this experiment.

simplicity, we will refer to the angle of polarizer by its effect on the photon beam and not by the literal angle of the half wave plate.

3. Results

Given Malus' Law, the expected coincidence rate of the detectors is proportional to $\cos^2(\alpha-\beta)$. To verify this, with β kept constant, the coincidence rate of the setup was measured over α.

By varying both α and β, two trials were conducted measuring the necessary coincidence rates to calculate S for $a = 0$, $b = 22.5$, $a' = 45$, and $b' = 67.5$. Each trial consisted of 16 total measurements, consisting of the four 4 measurements needed for $E(a, b)$, the 4 measurements needed for $E(a', b)$, the 4 measurements needed for $E(a, b')$, and the 4 measurements needed for $E(a', b')$. The data for both trials is tabulated in Table 1.

4. Analysis

The preliminary results for fixed β agree with Malus' Law, the experimental results fitting the curve $N(\alpha) = 50\cos^2(\alpha)$ with an R^2 value of .997, plotted in Figure 3. Finding N_{tot} for any E grouping from Table 1 results in approximately 100 incoming photons per second, for our setup. This is indicative of the reduction in intensity predicted by Equation 1.2, as $\frac{1}{2}N_{\text{tot}} = 50\,{}^{\text{counts}}/_{\text{s}} = \max(N(\alpha))$.

α (deg)	N(α)
0	51
5	47.2
10	40.2
15	36
20	28.6
25	20.8
30	12
35	7.8
40	3
45	0.4
50	1
55	7
60	9.6
65	20.2
70	28.4
75	36.2
80	41.4
85	46.6
90	49

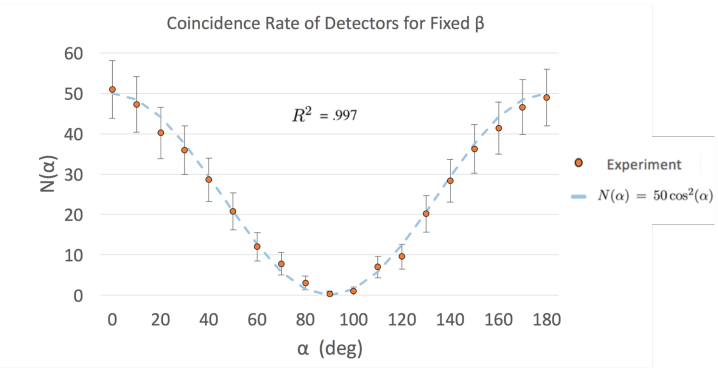

FIGURE 3. The coincidence rate of both detectors was recorded over various values of α at a constant $\beta = 0$. For each α, $N(\alpha)$ was measured over a 5 s interval and normalized to number of coincidences per second. The measured rate follows a curve proportional to $\cos^2(\alpha)$.

TABLE 1. Two trials were conducted investigating the coincidence of the two photon detectors for various values of α and β. We conducted two trials, $N_1(\alpha, \beta)$ and $N_2(\alpha, \beta)$, the outcomes of which are both displayed above. The experimental setup was disassembled and reassembled between trials.

Run	α (deg)	β (deg)	$N_1(\alpha, \beta)$	$N_2(\alpha, \beta)$
1	0	22.5	34	42
2	0	112.5	12	7
3	90	22.5	12	9
4	90	112.5	34	37
5	0	67.5	4	7
6	0	157.5	40	41
7	90	67.5	47	40
8	90	157.5	5	6
9	45	22.5	50	40
10	45	112.5	5	8
11	135	22.5	7	10
12	135	112.5	39	37
13	45	67.5	39	34
14	45	157.5	10	9
15	135	67.5	14	11
16	135	157.5	31	35

In Table 2, the values of E, and from them S, are calculated for each trial using Equations 1.3 and Equation 1.11, respectively. In both trials, S was found to be outside the allowable region for HVT. The expected value of S_{QM} was not attained by either trial; in both trials $S < S_{\mathrm{QM}}$. This can be explained by the finite time resolution of the single photon detectors. Any coincidences measured within a 25 ns window were counted, allowing for a nonzero probability of stray photons hitting our detectors. The overall effect of these randomly polarized coincidences is a reduction in the measurement of S.

TABLE 2. S is calculated per trial. In both trials, the error in S excludes the possibility of S being included within the region allowed by HVT.

	Trial 1	**Trial 2**
E(0,22.5)	.48±.09	.66±.08
E(0,67.5)	-.81±.06	-.72±.07
E(45,22.5)	.76±.06	.62±.08
E(45,67.5)	.49±.09	.55±.09
S	2.54±.16	2.56±.16

5. Conclusion

The theory of a local hidden variable governing the seemingly probabilistic behavior of quantum systems was disproven in this experiment. It follows from this result that multiple local hidden variables are also excluded, given that any configuration of variables can be mathematically modeled by a single variable with a probability distribution indicative of the outcomes of the collection of physical variables.

Globally hidden variables were not considered, as that would involve the analysis of functions such as $A(\alpha, \beta, \chi)$ and $B(\alpha, \beta, \chi)$, or some other incorporation of global variables. While excluded, it should be mentioned that globally hidden variables are widely regarded as unfavorable models. More favorable options for explaining quantum processes in a more determined nature exist in theories such as string theory or M-theory. However, testable features of such theories are hard to produce, given current experimental limitations. As such, these theories remain currently untestable in a manner as rigorous as the experiment conducted here.